Modification of STIM1 by *O*-linked *N*-Acetylglucosamine (*O*-GlcNAc) Attenuates Store-operated Calcium Entry in Neonatal Cardiomyocytes*[S]

Xiaoyuan Zhu-Mauldin[‡], Susan A. Marsh[§], Luyun Zou[¶], Richard B. Marchase[‡], and John C. Chatham[‡¶1]

From the [‡]Department of Cell Biology and [¶]Division of Molecular and Cellular Pathology, Department of Pathology, University of Alabama at Birmingham, Alabama 35294 and the [§]Program in Nutrition and Exercise Physiology, College of Pharmacy, Washington State University, Spokane, Washington 99210

Background: Increased cellular *O*-GlcNAc levels decrease store-operated Ca^{2+} entry (SOCE), however, the mechanism is not understood. STIM1 regulates SOCE, but effect of *O*-GlcNAc on STIM1 function is not known.
Results: Increased cardiomyocyte *O*-GlcNAcylation attenuated STIM1 puncta formation, SOCE and increased *O*-GlcNAc modification of STIM1.
Conclusion: *O*-GlcNAc modification of STIM1 plays a key role in regulating SOCE.
Significance: Protein *O*-GlcNAcylation regulates SOCE, a central Ca^{2+} signaling pathway.

Store-operated calcium entry (SOCE) is a major Ca^{2+} signaling pathway responsible for regulating numerous transcriptional events. In cardiomyocytes SOCE has been shown to play an important role in regulating hypertrophic signaling pathways, including nuclear translocation of NFAT. Acute activation of pathways leading to *O*-GlcNAc synthesis have been shown to impair SOCE-mediated transcription and in diabetes, where *O*-GlcNAc levels are chronically elevated, cardiac hypertrophic signaling is also impaired. Therefore the goal of this study was to determine whether changes in cardiomyocyte *O*-GlcNAc levels impaired the function of STIM1, a widely recognized mediator of SOCE. We demonstrated that acute activation of SOCE in neonatal cardiomyocytes resulted in STIM1 puncta formation, which was inhibited in a dose-dependent manner by increasing *O*-GlcNAc synthesis with glucosamine or inhibiting *O*-GlcNAcase with thiamet-G. Glucosamine and thiamet-G also inhibited SOCE and were associated with increased *O*-GlcNAc modification of STIM1. These results suggest that activation of cardiomyocyte *O*-GlcNAcylation attenuates SOCE via STIM1 *O*-GlcNAcylation and that this may represent a new mechanism by which increased *O*-GlcNAc levels regulate Ca^{2+}-mediated events in cardiomyocytes. Further, since SOCE is a fundamental mechanism underlying Ca^{2+} signaling in most cells and tissues, it is possible that STIM1 represents a nexus linking protein O-GlcNAcylation with Ca^{2+}-mediated transcription.

Store-operated calcium entry (SOCE) is a major Ca^{2+} signaling pathway responsible for regulating numerous transcriptional events. In cardiomyocytes SOCE has been shown to play an important role in regulating hypertrophic signaling pathways, including nuclear translocation of NFAT. Acute activation of pathways leading to *O*-GlcNAc synthesis have been shown to impair SOCE-mediated transcription and in diabetes, where *O*-GlcNAc levels are chronically elevated, cardiac hypertrophic signaling is also impaired. Therefore the goal of this study was to determine whether changes in cardiomyocyte *O*-GlcNAc levels impaired the function of STIM1, a widely recognized mediator of SOCE.

In non-excitable cells, store-operated calcium entry (SOCE),[2] also known as capacitive calcium entry (CCE), is widely recognized as a major Ca^{2+} signaling pathway responsible for regulating diverse transcriptional events (1, 2). The role of SOCE in mediating Ca^{2+} signaling in excitable cells such as cardiomyocytes is much less well accepted; however, in 2002, Marchase *et al.* demonstrated for the first time the presence of SOCE in neonatal rat ventricular myocytes (NRVMs) (3–5) and subsequently in adult cardiomyocytes (6). They also found that SOCE was required for activation of hypertrophic signaling pathways including nuclear translocation of NFAT by IP$_3$-generating agonists such as phenylephrine and angiotensin II. The integration of SOCE into accepted models of Ca^{2+} homeostasis, particularly in excitable cells, was hampered for many years by the lack of specific molecular effectors; however, STIM, Orai, and TRPC protein families have recently emerged as key mediators of this Ca^{2+} signaling pathway (7–15). In non-excitable cells STIM1 is localized to the endoplasmic reticulum (ER) membrane and depletion of ER Ca^{2+}, leads to a rapid conformational change in STIM1, resulting in puncta formation and translocation of STIM1 to ER/plasma membrane (PM) junctional regions (9, 16). Orai and TRPC calcium channels localized in the PM (7, 11–15), translocate to the ER/PM junction, in response to Ca^{2+} store depletion, where they interact with STIM1 triggering Ca^{2+} influx (17, 18). Although SOCE has not been widely studied in cardiomyocytes, recent studies have shown that STIM1-mediated SOCE plays an important role in cardiomyocyte hypertrophy in both neonatal cardiomyocytes and more recently the adult rat heart (19–23).

The *O*-linked attachment of β-*N*-acetyl-glucosamine (*O*-GlcNAc) to serine and threonine residues of nuclear and

[2] The abbreviations used are: SOCE, store-operated calcium entry; CCE, capacitive calcium entry; NRVM, neonatal rat ventricular myocytes; *O*-GlcNAc, *O*-linked β-*N*-acetyl-glucosamine; OGT, *O*-GlcNAc transferase; GlcNAcase, *N*-acetylglucosaminidase; HBP, hexosamine biosynthesis pathway; SERCA, sarcoplasmic reticulum Ca^{2+} ATPase; RyR, ryanodine receptor; GlcN, glucosamine; TMG, thiamet-G.

cytoplasmic proteins is rapidly emerging as a key mediator of numerous biological processes including transcription; translation; nuclear transport and cytoskeletal assembly. This atypical protein glycosylation takes place primarily in the cytosol and the nucleus, rather than the secretory pathway, and is regulated by the activities of two key enzymes, *O*-GlcNAc transferase (OGT) and *N*-acetylglucosaminidase (*O*-GlcNAcase). The levels of protein *O*-GlcNAcylation are also dependent on the metabolism of glucose via the hexosamine biosynthesis pathway (HBP), which leads to the formation of UDP-GlcNAc, the substrate for OGT and the essential sugar donor for *O*-GlcNAc formation. Acute activation of *O*-GlcNAc levels has been shown to be an endogenous stress response, and augmentation of this response increased tolerance of cells to stress, whereas its attenuation increased cell death (24). Conversely, sustained increases in *O*-GlcNAc have been implicated in a number of chronic diseases such as cancer, neurodegenerative diseases, diabetes and diabetic complications. Indeed, activation of the HBP and the resulting increase in *O*-GlcNAc levels have both been implicated in the adverse effects of diabetes on a variety of cells and tissues, including the heart. We recently reported that phenylephrine and angiotensin II induced hypertrophic signaling was blunted in cardiomyocytes from type-2 diabetic db/db mice, which was mediated at least in part by increased HBP flux and elevated protein *O*-GlcNAc levels (25).

Interestingly glucosamine, which increases HBP flux and leads to increased *O*-GlcNAc levels, inhibited SOCE in both J774 macrophages (26) and cardiomyocytes (3, 4); furthermore, hyperglycemia, which also increases HBP flux and *O*-GlcNAc levels has been shown to inhibit SOCE in both vascular smooth muscle cells (27) and cardiomyocytes (4). Of note, in cardiomyocytes the attenuation of SOCE and subsequent hypertrophic signaling was reversed by inhibition of glucose entry into the HBP (4). Furthermore, Nagy *et al.* reported that angiotensin II-induced increase in Ca^{2+} could be attenuated by increasing cardiomyocyte *O*-GlcNAc levels either by inhibiting *O*-GlcNAcase or by increasing the HBP with glucosamine (28).

Taken together these data support the notion that activation of cardiomyocyte *O*-GlcNAcylation attenuates SOCE. Therefore, given the central role of STIM1 in mediating SOCE, we postulated that increased *O*-GlcNAc levels would inhibit STIM1-mediated Ca^{2+} entry and further that STIM1 itself would be a target for *O*-GlcNAcylation and that this would be associated with decreased activation of STIM1.

EXPERIMENTAL PROCEDURES

All animal experiments were approved by the University of Alabama at Birmingham Institutional Animal Care and Use Committee and conformed to the Guide for the Care and Use of Laboratory Animals, published by the National Institutes of Health (NIH Publication No. 85-23, revised 1996).

Reagents and Plasmids—All reagents were purchased from Sigma, unless stated otherwise. Calcium chloride, magnesium chloride, and potassium chloride were purchased from Fisher Scientific (Pittsburgh, PA). Thiamet-G was from SD ChemMolecules LLC (Owings Mills, MD). Thapsigargin and culture medium products were purchased from GIBCO Invit-

rogen (Grand Island, NY). Both adenoviruses, YFP-STIM1 and mCherry-Orai1, were from Vector Biolabs (Philadelphia, PA).

Immunohistochemistry—Hearts were perfused as previously described (29, 30), and then perfusion-fixed with 4% paraformaldehyde, stored in 70% ethanol until paraffin embedding, and sectioned at 5 μm before being mounted on slides; deparaffinized in xylene; rehydrated in ethanol; and blocked with 5% goat serum in 1% bovine serum for 1 h at room temperature. Sections were incubated with primary antibodies against STIM1 (1:50; LB-B1880, LifeSpan BioSciences, Seattle, WA), sarcoplasmic/endoplasmic reticulum calcium-ATPase 2 (SERCA, 1:400; PA1–21904, Thermo Fisher Scientific, Rockford, IL), and ryanodine receptor 2 (RyR, 1:50; ARR-002, Alomone Labs, Jerusalem, Israel) diluted in 5% goat serum in 1% bovine serum overnight at 4 °C; appropriate secondary antibodies conjugated to either Alexa Fluor 488 (green) or 594 (red) (Invitrogen, Carlsbad, CA) were used to visualize the specific proteins, with 4′,6-diamidino-2-phenylindole (DAPI; blue) to identify nuclei. Midwall sections of the left ventricular free wall were examined and image acquisition was performed on a Zeiss Axioplan 2 epifluorescence microscope with an AxioCam MRm cooled CCD camera and AxioVision software (Carl Zeiss Microimaging, Thornwood, NY). Linescans to detect intracellular patterns of *O*-GlcNAc distribution were generated using ImageJ software (National Institutes of Health, Bethesda, MD).

Membrane Fractionation—For preparation of the membrane compartment, heart tissue was homogenized in ice-cold lysis buffer containing, in mM: 20 Tris (pH 7.4), 5.0 EDTA, 250 sucrose, 1.0 phenylmethanesulfonyl fluoride, and 2.5% protease inhibitor mixture. Tissue homogenates (20% w/v) were centrifuged at $1,000 \times g$ for 10 min to remove nuclei and debris, and the supernatant was ultracentrifuged at $110,000 \times g$ for 75 min at 4 °C to pellet the crude membrane fraction (both the sarcolemmal and microsomal subfractions). The resulting pellet was resuspended in solubilization buffer (50 mM Tris (pH 7.4), 100 mM sodium chloride, 50 mM lithium chloride, 5 mM EDTA, 0.5% (v/v) Triton X-100, 0.5% (w/v) sodium deoxycholate, 0.05% (w/v) SDS, and 0.02% (w/v) sodium azide) using a glass homogenizer. After incubation for 30 min on ice, the remaining insoluble material was collected by centrifugation ($14,000 \times g$, 10 min, 4 °C). Equal protein amounts of the supernatant (particulate membrane fraction) were suspended in 2× Laemmli buffer (Bio-Rad), boiled for 5 min, and then immunoblotted and visualized as described below. Anti-Pan-cadherin, -SERCA, and -GAPDH antibodies (Abcam, Cambridge, MA) were used to verify the purity of membrane, the abundance of ER membrane in the membrane fractions and cytoplasmic fractions, respectively.

Neonatal Rat Ventricular Myocyte Primary Culture and Infection—Primary cultures of neonatal rat ventricular myocytes (NRVMs) were obtained from 2–3-day-old neonatal Sprague-Dawley rats and cultured as described previously (3, 31). NRVMs were grown on collagen-coated plates in culture growth medium containing 15% fetal bovine serum (FBS) on the first day. On the next day, medium was replaced, and cells were grown in culture growth medium without FBS. Within 1–2 days of isolation, a confluent monolayer of spontaneously beating NRVMs had formed. On the third day after isolation,

NRVMs were infected with an adenovirus encoding enhanced yellow fluorescent protein linked to STIM1 (eYFP-STIM1, 2 moi) with or without another adenovirus encoding one of the fruit fluorescent proteins, mCherry, linked to Orai1 (mCherry-Orai1, 5 moi). After overnight infection, cells were subjected to SOCE stimulation as described below.

Immunoprecipitation and Immunoblot—Heart tissue (10 mg) was homogenized in 1 ml of T-PER (Pierce) supplemented with 40 μM PUGNAc (Toronto Research Chemicals, North York, Ontario, Canada), 1 mM sodium orthovanadate, 20 mM sodium fluoride, and 5% protease inhibitor mixture and lysed for 60 min on ice. Cultured NRVMs were lysed for 30 min on ice with 1× RIPA buffer (50 mM Tris·HCl, pH 8.0, 150 mM NaCl, 1% (v/v) Nonidet P-40, 0.5% (w/v) sodium deoxycholate, 1 mM EDTA, and 0.1% SDS] containing 2% protease inhibitor mixture (Sigma) and 40 μM PUGNAc, at the end of thapsigargin (5 mM) plus EGTA (2 mM) treatment. Consistent with our earlier studies, PUGNAc was present throughout the lysis protocol to inhibit *O*-GlcNAcase, thereby preventing loss of *O*-GlcNAc (32).

Lysed proteins from heart tissue or NRVMs were harvested by centrifuging at 15,000 × g for 15 min, and protein concentration of the supernatant was assessed using the Bio-Rad Protein Assay Kit (Bio-Rad). Samples containing equal amount of protein (1000 μg for tissue and 500 μg for NRVMs) were mixed with polyclonal rabbit anti-STIM1 antibody (#4916, Cell Signaling, 1:50) or anti-GFP antibody (ab6556, Abcam, 1:250) overnight at 4 °C with protein A-agarose beads (Upstate). The agarose beads then were washed three times in PBS containing 1% Nonidet P-40 followed by three additional washes with PBS. Antigens were eluted from the beads and boiled for 5 min in Laemmli buffer prior to SDS-PAGE. Immunoblots were incubated with anti-Orai1 (#1280, Cell Signaling, 1:500), anti-O-GlcNAc (CTD 110.6, Mary-Ann Accavitti, UAB Epitope Recognition and Immunoreagent Core, 1:1000), anti-phospho-MAPK/CDK substrates (#2325, Cell Signaling, 1:1000), anti-STIM1 (1:1000) and/or anti-GFP (1:5000) antibodies for overnight at 4 °C, followed by incubation with appropriate secondary antibodies and chemiluminescence visualization.

Fluorescence Imaging—NRVMs were plated at a density of 100–400 cells/mm^2 on eight-well slide chambers (NUNC) and were infected with an eYFP-STIM1 or mCherry-Orai1 adenovirus 24 h prior to imaging studies. Cells were then pre-treated with or without glucosamine or thiamet-G (an OGA inhibitor) for 1 h, washed with HBSS (H8264, Sigma) and CaCl$_2$ (1.2 mM) and MgSO$_4$ (1.0 mM) for three times, then stabilized in HBSS plus CaCl$_2$ and MgSO$_4$ for 30 min at room temperature. Live imaging was performed on a Zeiss LSM710 confocal laser-scanning microscope through a 20× objective lens. Images were taken every 5 s with 37 or 97 cycles in total. Thapsigargin (5 mM) plus EGTA (2 mM) were added between 4th and 5th cycle to induce STIM1 puncta formation. For dose-response experiments, cells were cultured on the slides, pre-treated with glucosamine at 0, 50 μM, 100 μM, 0.5 mM, 1 mM, 5 mM, or 10 mM or thiamet-G at 0, 0.01 μM, 0.1 μM, 0.5 μM, 1 μM, or 5 μM for 1 h, washed three times with HBSS, then treated with thapsigargin in Ca^{2+}-free HBSS for 4 min. Cells were fixed with PLP fixative

(2% paraformaldehyde, 0.075 M lysine, 0.037 M sodium phosphate, 0.01 M periodate) for 30 min, washed with PBS for 3 times, mounted to microscope slide with Vectashield® Mounting Medium (Vector Laboratories), sealed upside-down on the cover slide with nail polish and dried at room temperature before imaging. The data were collected and analyzed using light ZEN Elite and ImageJ.

STIM1 puncta were analyzed using the "Analyze Particles" feature in ImageJ. Briefly, after background subtraction, fluorescent images are converted into a binary mask and puncta were identified based on their relative intensity, compared with background, size, and circularity.

Intracellular Ca^{2+} Measurements—NRVMs were pretreated with or without glucosamine or thiamet-G for 1 h prior to loading with Fluo-4 AM (1μM, F-14201, Invitrogen) for 45 min, washed three times, then stabilized in HBSS plus CaCl$_2$ and MgSO$_4$ for 30 min. Digital images were obtained in room-temperature HBSS plus CaCl$_2$ and MgSO$_4$ using a Zeiss LSM710 confocal laser-scanning microscope. Images were taken every 15 s for 6 min to visualize KCl-activated Ca^{2+}/Sr^{2+} entry or 12min for thapsigargin-activated Ca^{2+} entry. During imaging, the cells were treated with EGTA (2 mM) first for ~2 min, stimulated with thapsigargin (5 μM) for ~6 min and 1.2 mM Ca^{2+} was then added back for 4 min. To test the permeability of Sr^{2+}, SrCl$_2$ was applied instead of CaCl$_2$ for close to 2min; then Ca^{2+} was added back for 2min. For KCl-activated Ca^{2+}/Sr^{2+} entry, KCl (30 mM) plus SrCl$_2$ (1.2 mM) or CaCl$_2$ (1.2 mM) was added for 4 min after EGTA treatment. The fluorescence intensity was normalized to the initial fluorescence; thus the normalized fluorescence is reported as F/F$_0$. The data were collected and analyzed using light ZEN Elite and ImageJ (version 1.44).

Data Analysis—All data are expressed as mean ± S.E. Comparisons were performed with Student's *t* test or one-way ANOVA followed by Dunnett or Tukey's multiple comparison test as indicated in the figure legends. Statistically significant differences between groups were defined as p < 0.05 and are indicated in the figure legends.

RESULTS

STIM1 and Orai1 Are Expressed in the Adult Rat Hearts— STIM1, sarcoplasmic reticulum Ca^{2+} ATPase (SERCA) and ryanodine receptor (RyR) were all present throughout the left and right ventricles; however, to better visualize the striated nature of the SR the images and analyses presented in Fig. 1*A* were derived from the midwall of the left ventricular free wall. We show that STIM1 is not only present in the adult rat heart, but also that it is co-localized with both SERCA and RyR, consistent with it being localized to the SR. In Fig. 1*B* it is clear that both STIM1 and Orai1 proteins are present in the membrane fractions entirely consistent with data in non-excitable cells.

STIM1 Forms Puncta and Interacts with Orai1 upon SOCE Activation in NRVMs—To better characterize STIM1 function in cardiomyocytes, NRVMs were transfected overnight with eYFP-STIM1 adenovirus and/or mCherry-Orai1 adenovirus and live cell imaging performed before and after treatment of cells with thapsigargin and EGTA to deplete SR/ER Ca^{2+} stores. Under resting conditions STIM1 was present in distrib-
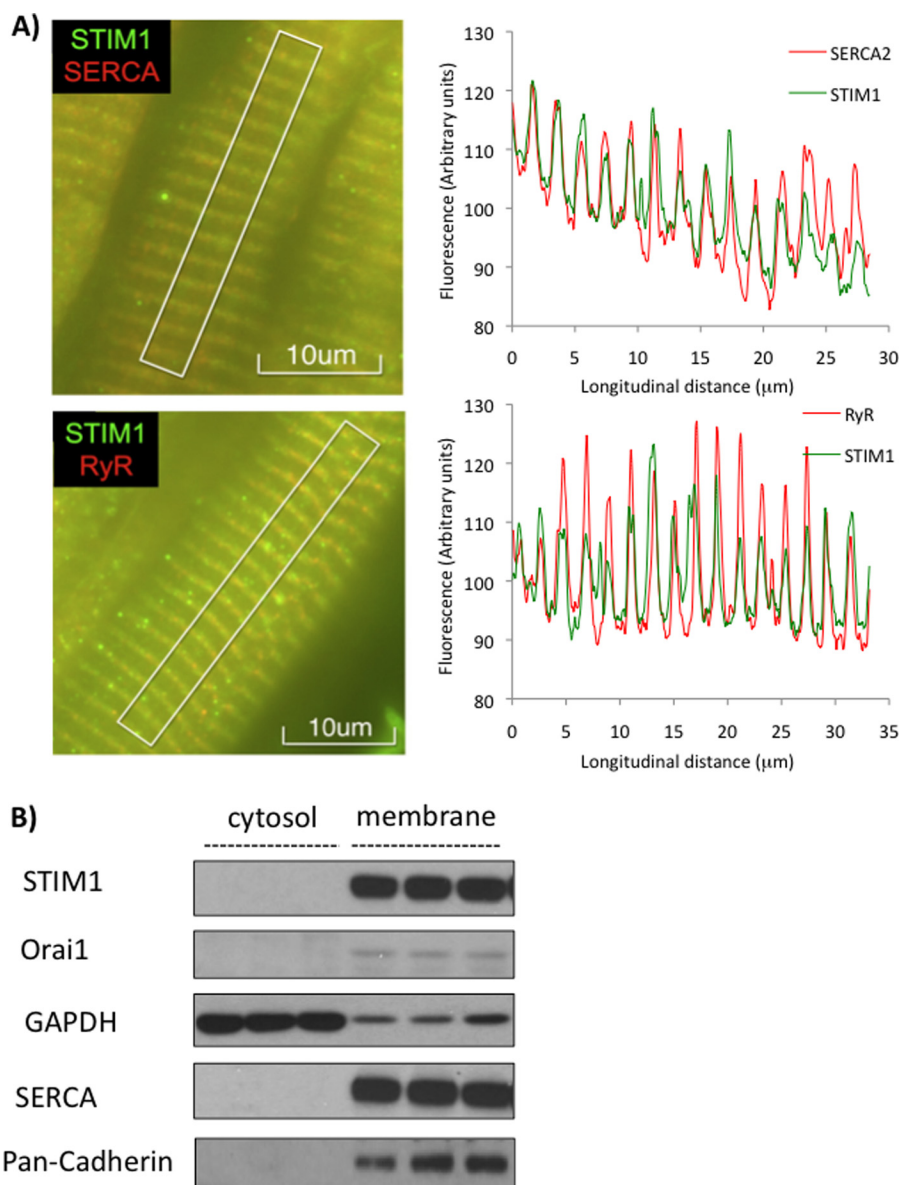
FIGURE 1. **STIM1 in the adult rat heart.** *A*, *left*: images of perfusion-fixed adult rat heart following immunohistochemical antibody staining showing co-localization of STIM1 (*green*) with both SERCA2 and RyR consistent with SR localization in the midwall of the left ventricular free wall; *Right*: image analysis of fluorescent intensities confirming co-localization of STIM1 with SERCA2 and RyR. *B*, representative STIM1 and Orai1 immunoblots from crude membrane fraction of whole heart extracts.

uted reticular fashion, consistent with SR/ER localization; however, following thapsigargin/EGTA the appearance of intense spots or puncta were readily observed within 1 min reaching a steady state within ~3 min (Fig. 2*A*, and supplemental Fig. S1). Similarly in NRVMs transfected with mCherry-Orai1, thapsigargin/EGTA stimulated the formation of Orai1 puncta along the membrane and this also co-localized with STIM1 puncta formation (Fig. 2*B*). It should be noted that the imaging experiments were performed at room temperature, consequently, the kinetics of STIM1 puncta formation were slower and therefore more easily visualized than if studied at 37 °C. Thus, these data demonstrate that in NRVMs, consistent with studies in non-excitable cells, ER/SR Ca^{2+} store depletion induces the dynamic STIM1 puncta formation and the interaction between STIM1 and Orai1.

Activation of Protein O-GlcNAc Levels Attenuates STIM1 Aggregation—We have previously demonstrated that SOCE is attenuated when protein O-GlcNAc levels are elevated by increasing flux through the HBP (3, 4, 28); therefore, we postulated that increased protein *O*-GlcNAcylation would blunt STIM1 puncta formation. To increase *O*-GlcNAc levels, we used glucosamine, which increases *O*-GlcNAc synthesis, and thiamet-G, a highly specific *O*-GlcNAcase inhibitor (33), which blocks *O*-GlcNAc removal. In Fig. 3 we show the effects of 1 h pretreatment with either glucosamine (5 mM) or thiamet-G (10 μM) on STIM1 puncta formation induced by thapsigargin and EGTA. In the control group, ~95% of NRVMs became STIM1 puncta positive within 3 min; however, this was significantly attenuated by treatment with either glucosamine or thiamet-G (Fig. 3*B*). The average number of puncta per cell also signifi-
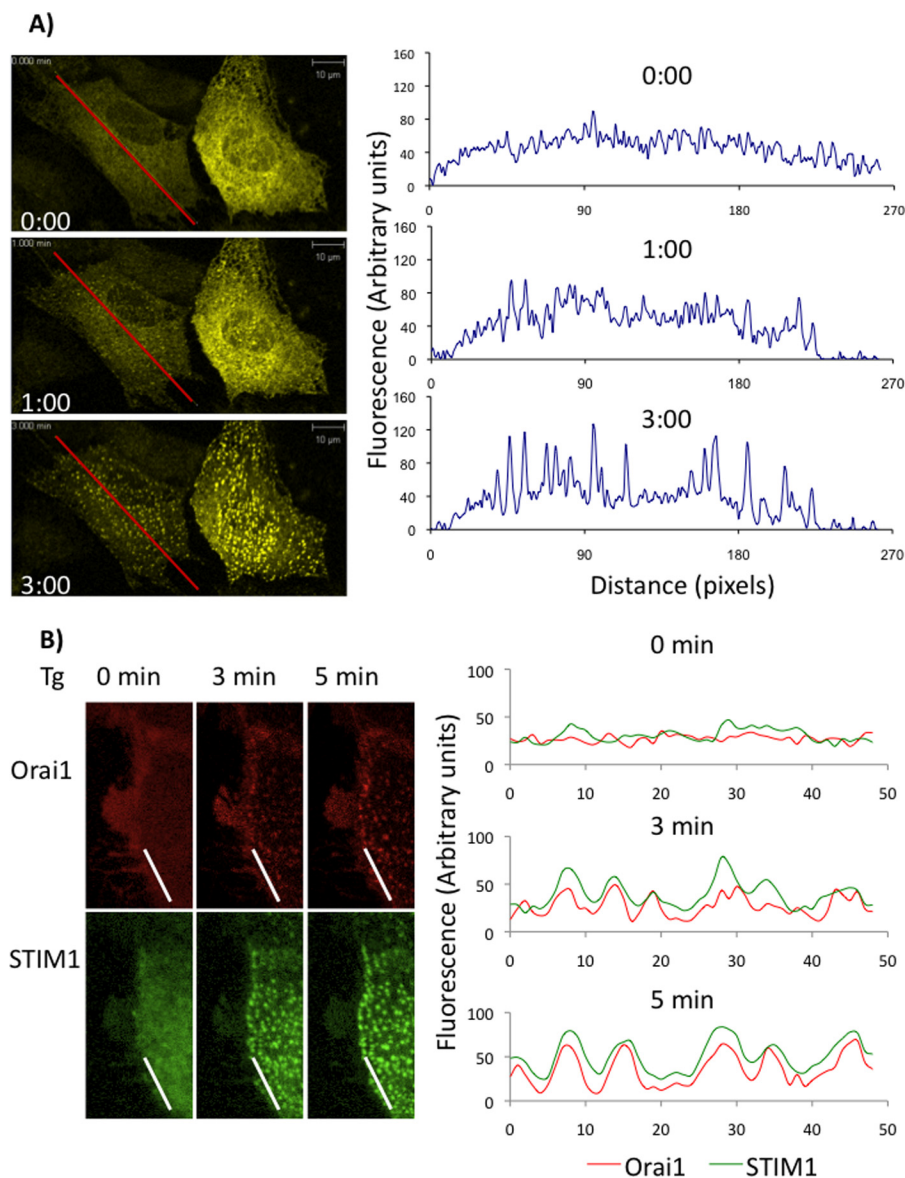
FIGURE 2. **STIM1 forms puncta and interacts with Orai1 in NRVMs.** *A*, eYFP-STIM1 infected NRVMs were treated with thapsigargin (TG, 5 μM) plus EGTA (2 mM) to deplete ER/SR Ca^{2+}. *Left* images from before (0 min) and at 1 and 3 min after treatment are shown. Images were recorded for up to 8 min following treatment, with 5 s intervals and a total of 97 cycles. *Right:* image analysis of fluorescent intensities along the line as indicated at 0, 1, and 3 min, showing the changes in intensities from diffuse at 0 min to puncta at 3 min. *B*, NRVMs, with combined YFP-STIM1 and mCherry-Orai1 infection overnight, followed by treated with thapsigargin (TG, 5 μM) plus EGTA (2 mM) to deplete ER/SR Ca^{2+}. *Left:* images of STIM1 and Orai1 from before (0 min) and at 3 and 5min after treatment are shown. *Right:* image analysis of fluorescence intensities along the line as indicated indicating co-localization of STIM1 and Orail1 following treatment.

cantly decreased from 60 $\pm$ 7 to 27 $\pm$ 3 with glucosamine or 25 $\pm$ 5 with thiamet-G treatment (Fig. 3*C*); however, puncta size was unaffected (Fig. 3*D*).

To assess whether the attenuation of STIM1 puncta formation by glucosamine and thiamet-G might be mediated by increasing protein *O*-GlcNAc levels we performed dose response experiments for both puncta formation and protein *O*-GlcNAc levels (Fig. 4). We found that glucosamine exhibited an EC_{50} of $\sim$214 μM for inhibiting STIM1 puncta formation (Fig. 4*A*) and EC_{50} of $\sim$164 μM for increasing overall protein O-GlcNAcylation (Fig. 4, *C* and *E*). As anticipated Thiamet-G was effective at much lower concentrations exhibiting an EC_{50} of $\sim$104 nM for inhibiting puncta formation (Fig. 4*B*) and EC_{50} of $\sim$70 nM for increasing overall protein *O*-GlcNAcylation (Fig. 4, *D* and *F*). The similarity between the EC_{50} for inhibiting

STIM1 puncta formation and increasing *O*-GlcNAc levels provides strong support for the notion that the attenuation of STIM1 puncta formation by glucosamine and thiamet-G are mediated, at least in part by the increase in protein *O*-GlcNAc levels.

Increased Protein O-GlcNAcylation Attenuates SOCE but Not Voltage-gated Ca^{2+} Entry—In Fig. 5*A* we show that, consistent with attenuating STIM1 puncta formation, both glucosamine and thiamet-G significantly blunted subsequent Ca^{2+} entry. Since NRVMs also contain voltage-gated Ca^{2+} entry pathways, we assessed whether increasing O-GlcNAc levels would also attenuate this Ca^{2+} entry pathway. We confirmed that this is also the case, since pre-treatment with glucosamine had no effect on the increase in Ca^{2+} that occurred by depolarizing the cells with high K^+ (Fig. 5*B*). This is also entirely con-
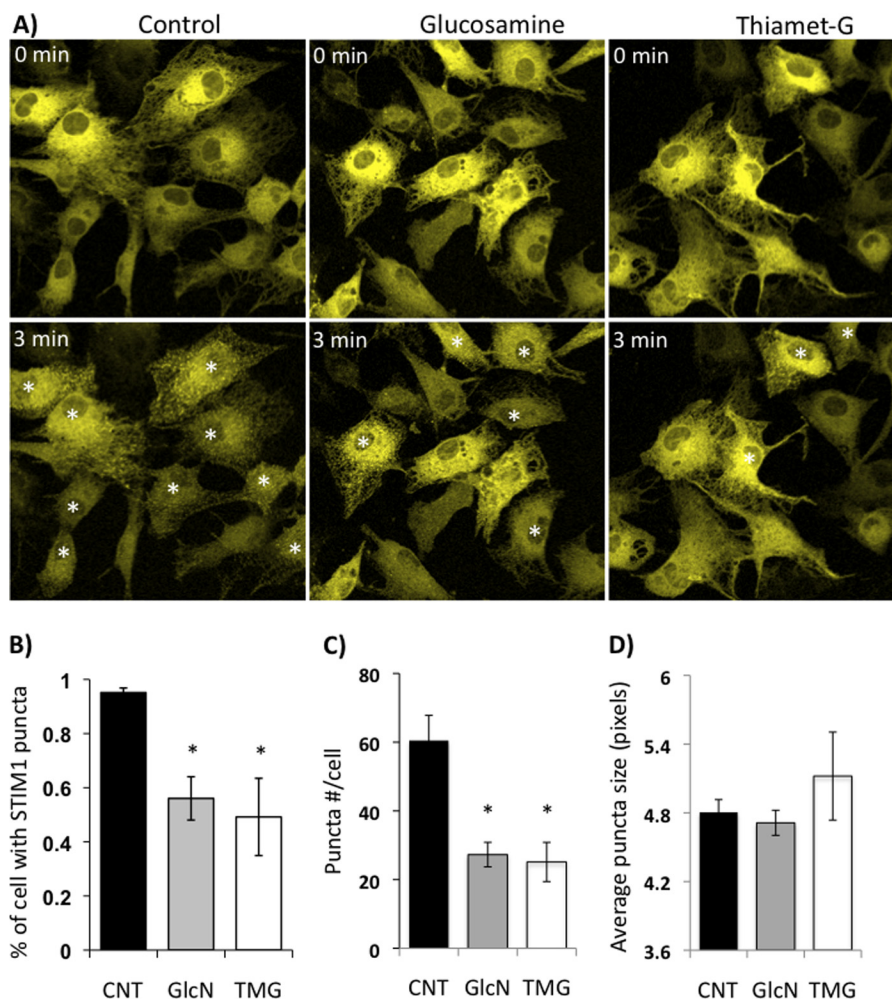
FIGURE 3. **STIM1 puncta formation was blunted by glucosamine or thiamet-G treatment.** *A*, fluorescent images of NRVMs with eYFP-STIM1 transfection overnight before (0 min) and 3 min following treatment with thapsigargin (5 μM) plus EGTA (2 mM) to deplete ER/SR Ca^{2+}. Cells received either no pretreatment (Control) or 1 h pretreatment with glucosamine (5 mM, *GlcN*) or Thiamet-G (10 μM, *TMG*). *B*, percentage of cells with STIM1 puncta 3 min following thapsigargin treatment. Data from 4 cultures, 4 or 6 biological repeats for each treatment from each culture and $\sim$50 cells were counted for each repeat. *, $p < 0.05$ *versus* CNT, one-way ANOVA with Dunnett's multiple comparison test. *White asterisks* indicate puncta positive cells. *C*, average STIM1 puncta number per cell and *D*, average puncta size 3 min following thapsigargin treatment. $N \geq 5$; * $p < 0.05$ *versus* CNT, Student's *t* test.

sistent with other studies demonstrating that acute increases in cardiac *O*-GlcNAc levels had no effect on contractile function, which is mediated by voltage-gated L-type Ca^{2+} channels (29, 30, 34, 35).

SOCE mediated by STIM1 has been reported to involve interaction with TRPC as well as Orai1 (7, 15, 36, 37). However, it has been reported that TRPCs are relatively non-selective Ca^{2+} channels (38), whereas Orai1 is Ca^{2+} selective (10, 39, 40). Therefore to better characterize SOCE in cardiomyocytes, we examined its divalent cation selectivity by taking advantage of the fact that Sr^{2+} interacts with Fluo-4 in a similar manner to Ca^{2+}. In Fig. 5*C* we demonstrate that consistent with previous studies (41), activation of voltage-gated Ca^{2+} entry resulted in influx of Sr^{2+}. These data also indicate that Fluo-4 has a similar sensitivity to both Sr^{2+} and Ca^{2+}. In Fig. 5*D* we show that following store depletion the addition of Sr^{2+} results in a relatively small increase in fluorescence; whereas, the subsequent addition of Ca^{2+} resulted in an increase in fluorescence similar to that seen when Ca^{2+} alone was added. These data are consistent with the studies from Voelkers *et al.* (21), and demon-

strate that in NRVMs, SOCE is Ca^{2+}-selective, thus predominantly mediated by Orai1, rather than TRPCs.

Therefore, consistent with the original studies of SOCE in cardiomyocytes (6), these data demonstrate that both STIM1-mediated SOCE and voltage-gated Ca^{2+} entry pathways co-exist in NRVMs and that the effect of increased *O*-GlcNAcylation is specific for SOCE. It is also evident that STIM1-mediated SOCE is more selective for Ca^{2+} than voltage-gated Ca^{2+} entry, supporting the notion that it is predominantly mediated by STIM1-Orai1 coupling.

STIM1 Is a Target for O-GlcNAcylation—The results above demonstrate an association between increased cellular *O*-GlcNAc levels and decreased STIM1 puncta formation; therefore, to determine if STIM1 itself was a target for *O*-GlcNAcylation, we immunoprecipitated endogenous STIM1 from control and glucosamine treated NRVMs followed by an anti-*O*-GlcNAc immunoblot. As shown in Fig. 6*A*, there were multiple *O*-GlcNAc positive bands from both control and glucosamine-treated groups, with a particularly intense band at the appropriate molecular weight for STIM1; further, the inten-
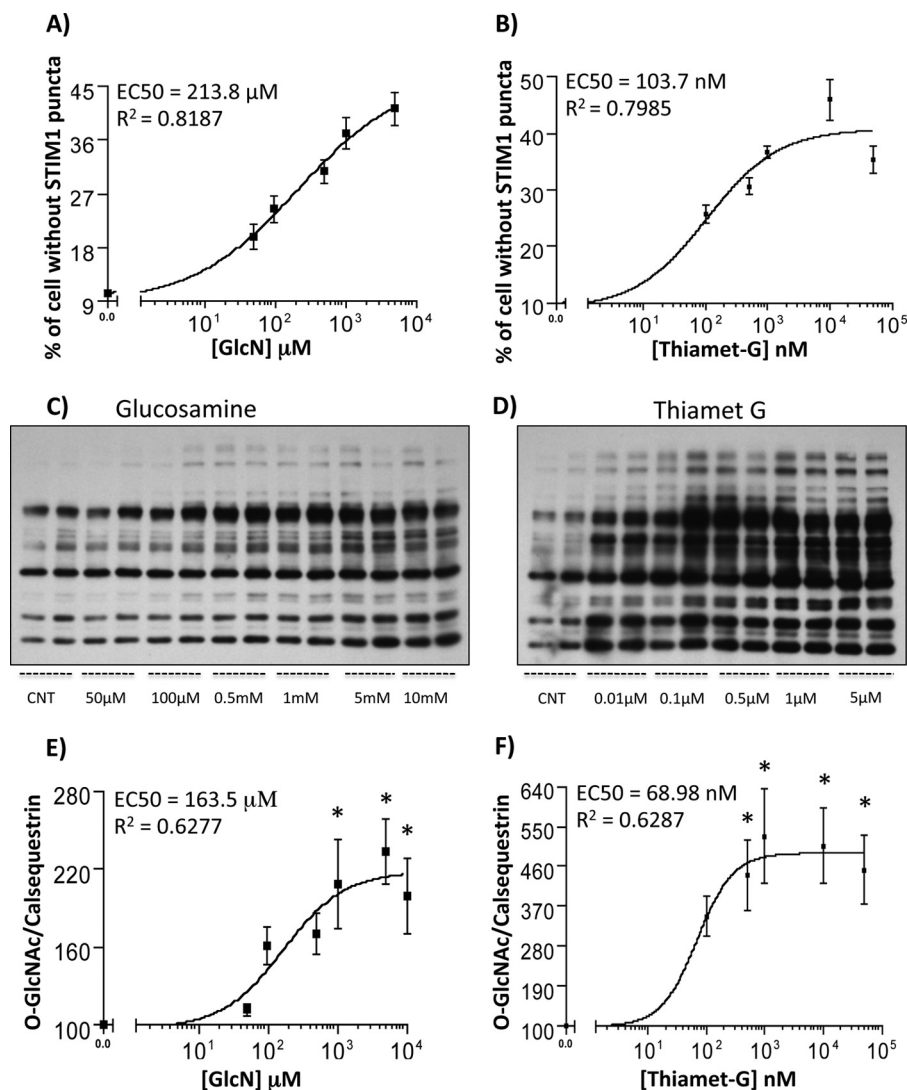
FIGURE 4. **Dose response curves for glucosamine and thiamet-G treatment on inhibiting STIM1 puncta formation and increasing protein *O*-GlcNAc levels.** EC_{50} curves for *A*) GlcN and *B*) TMG on inhibition of STIM1 puncta formation. Data from 5– 6 independent cultures with 2– 4 biological repeats for each culture and >100 cells counted for each repeat. Representative *O*-GlcNAc immunoblots from NRVMs were incubated with *C*) glucosamine or *D*) thiamet-G for 1 h at the indicated concentrations. EC_{50} curves for *E*) glucosamine and *F*) thiamet-G on increasing *O*-GlcNAc levels, assessed by densitometric analysis followed by normalization to calsequestrin levels (not shown). $n = 3$. *, $p < 0.05$ *versus* control, one-way ANOVA with Dunnett's multiple comparison test.

sity of *O*-GlcNAc staining was higher in the glucosamine-treated groups. It can also be seen that the addition of 10 mM GlcNAc markedly attenuated the *O*-GlcNAc-positive bands, including the intense STIM1 band, confirming the specificity for O-GlcNAcylation (Fig. 6*B*). We subsequently, determined the effect of thiamet-G and thapsigargin on *O*-GlcNAc levels in NRVMs and found that, while thiamet-G treatment significantly increased STIM1 *O*-GlcNAcylation by ~2.5-fold (Fig. 6*C*), thapsigargin treatment had no effect (Fig. 6*D*).

It has been reported that ERK1/2 mediated STIM1 phosphorylation is required for SOCE activation in HEK293 cells (42); in Fig. 6*D* we demonstrate that in NRVMs STIM1 phosphorylation is also significantly enhanced by thapsigargin treatment. Interestingly, with thiamet-G pretreatment, there was a significant increase in basal STIM1 phosphorylation, but there was no further increase with thapsigargin (Fig. 6*E*).

DISCUSSION

Evidence is accumulating that SOCE pathways are present in excitable cells such as cardiomyocytes and contributes to the activation of key Ca^{2+}-sensitive pathways such as activation of NFAT-mediated transcription (3, 6), similar to the accepted function of SOCE in non-excitable cells (12). Although an increasing number of proteins have been implicated in the regulation of SOCE (43), it is widely accepted that STIM1 is essential for activation of SOCE (12). Our earlier studies have shown that increased HBP flux and/or protein *O*-GlcNAcylation was associated with decreased SOCE in both excitable and non-excitable cells (3, 4, 26, 29). Here, we demonstrate that increased *O*-GlcNAcylation prevented STIM1 puncta formation, blunted STIM1-mediated SOCE, as well as increasing *O*-GlcNAc modification of STIM1; these results provide a critical link between regulation of cellular *O*-GlcNAcylation and Ca^{2+} signaling. Given the broad role of SOCE in mediating
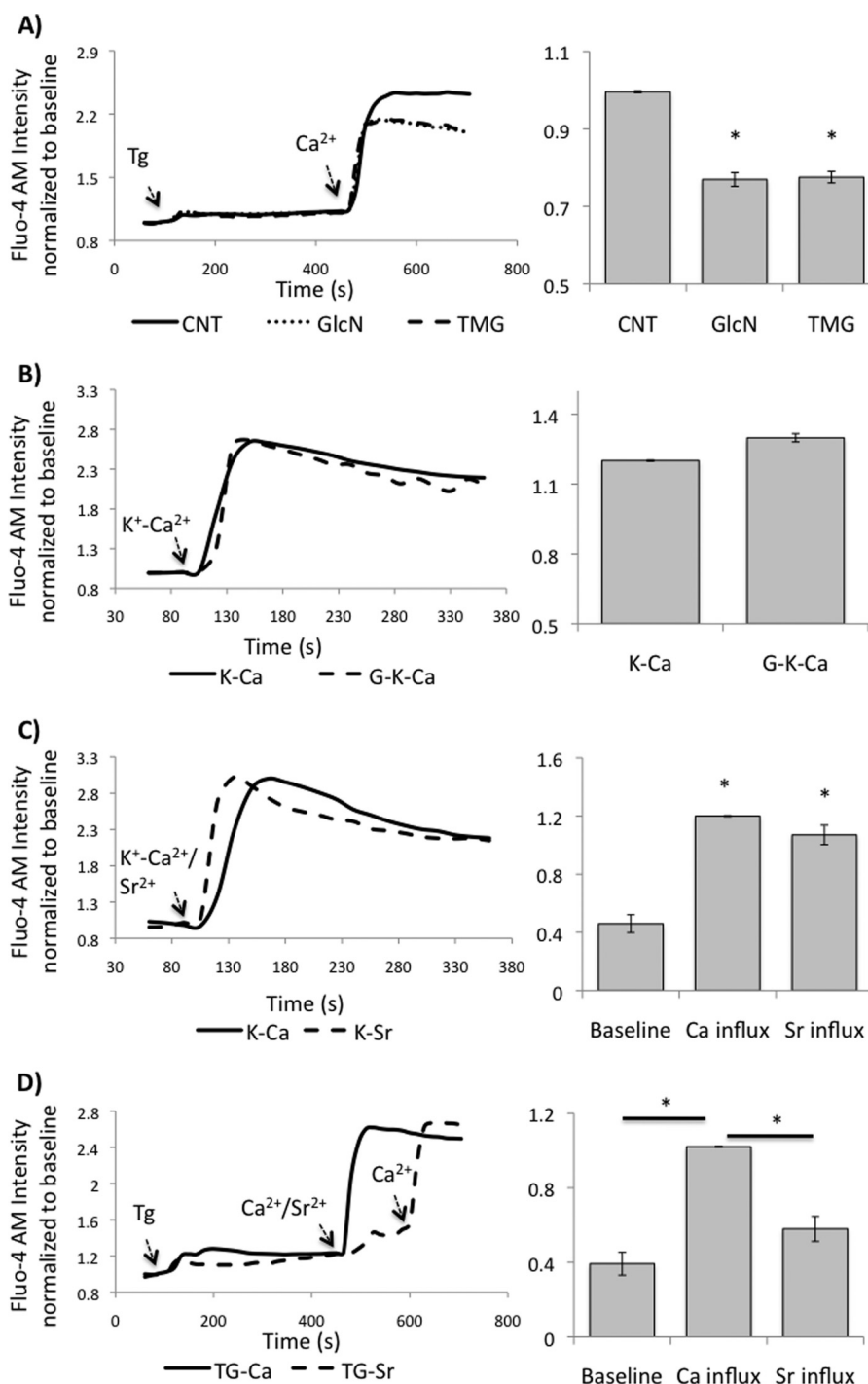
FIGURE 5. *A*, effects of glucosamine and thiamet-G on SOCE. NRVMs were pretreated with or without GlcN or TMG. *Left panel*: representative fluorescence intensity traces from a group of NRVMs before and after thapsigargin treatment followed by Ca^{2+} addition; *Right panel:* average peak fluorescence intensity normalized to untreated Controls (CNT); *B*, effect of glucosamine on voltage-gated Ca^{2+} entry. Following pretreatment with or with glucosamine NRVMs were depolarized by increasing K^+ concentration. *Left panel*: representative fluorescence intensity traces before and after depolarization; *Right panel:* average peak fluorescence intensity normalized to mean intensity at the end of recording period; *C*, activation of voltage gated Ca^{2+} pathways facilitates both Sr^{2+} and Ca^{2+} transport. *Left panel*: representative fluorescence intensity traces before and after depolarization; *Right panel:* average peak fluorescence intensity normalized to mean intensity at the end of recording period. *D*, activation of SOCE pathways facilitates Ca^{2+} but not Sr^{2+} entry. Data are mean ± S.E. from 3–4 independent cultures, with at least 3 biological repeats for each culture, and ~50 cells counted for each repeat. Cells were loaded with Fluo-4 AM for 45 min, washed with HBSS for three times, and stabilized at room temperature for 30 min. Images were taken every 15 s for 6 min. *, $p < 0.05$ *versus* CNT or baseline or as indicated.

Ca^{2+}-dependent transcriptional events in numerous cell types, these data provide a new mechanism by which *O*-GlcNAcylation contributes to regulation of cellular function.

In excitable cells such as cardiomyocytes the predominant view of Ca^{2+} signaling is that it is regulated either via voltage-dependent Ca^{2+} entry pathways or IP_3-induced Ca^{2+} release from intracellular stores, such as SR/ER (44). However, Marchase *et al.* clearly showed that SOCE was present in cardiomyocytes and indeed played a key role in agonist induced hypertrophic signaling including activation of NFAT-mediated
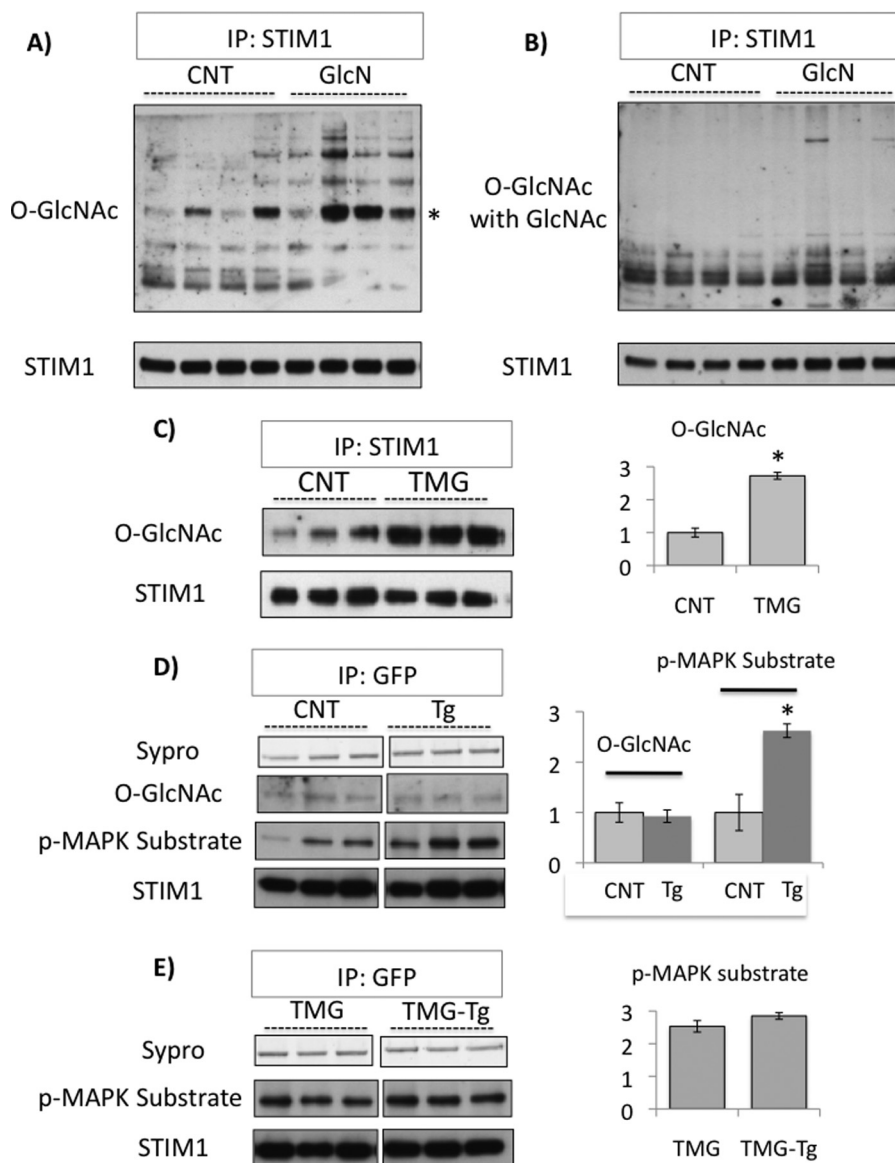
FIGURE 6. *A*, NRVMs untreated or treated with glucosamine (5 mM, GlcN) for 1 h followed by STIM1 immunoprecipitation (*IP*) and *O*-GlcNAc immunoblot; * indicates the STIM1 band; *B*, same as *A*, but with the addition of 10 mM GlcNAc during *O*-GlcNAc immunoblot; *C*, NRVMs untreated or treated with thiamet-G (1 μM, TMG) for 1 h followed by STIM1 immunoprecipitation (IP) and *O*-GlcNAc or STIM1 immunoblot (*left panel*). Ratio of *O*-GlcNAcylation/STIM1 intensity normalized to CNT, *, $p < 0.05$ *versus* CNT, Student's *t* test (*right panel*); *D*, NRVMs with E-YFP-STIM1 transfection and untreated or treated with or without thapsigargin (TG, 5 μM) plus EGTA (2 mM) for 5 min, followed by GFP immunoprecipitation (*IP*) and *O*-GlcNAc, phospho-MAPK/CDK substrate or STIM1 immunoblot (*left panel*). Ratio of *O*-GlcNAc/STIM1 and phospho-MAPK/CDK substrate/STIM1 intensity normalized to CNT, *, $p < 0.05$ *versus* CNT, Student's *t* test (*right panel*); *E*, same as *D* but with 1 h of thiamet G (1 μM, *TMG*) pretreatment, followed by GFP immunoprecipitation (*IP*) and phospho-MAPK/CDK substrate or STIM1 immunoblot (*left panel*). Ratio of phospho-MAPK/CDK substrate/STIM1 intensity normalized to CNT from *D* (they are from same immunoblot).

transcriptional pathways (3). More recently others have shown that STIM1-mediated SOCE was involved in cardiomyocyte hypertrophic signaling at the cellular level (21) and that *in vivo*, increased STIM1 levels are associated with pathological hypertrophy (19, 20). Taken together, these studies demonstrate growing support for the notion that STIM1-mediated SOCE plays a key role in cardiomyocyte Ca^{2+} signaling; however, little is known about the acute regulation of STIM1 function in cardiomyocytes. Prior to STIM1 being identified as one of the molecular mediators of SOCE, hyperglycemia and glucosamine were shown to attenuate SOCE in both macrophages and cardiomyocytes; furthermore, inhibition of the HBP reversed the effects of hyperglycemia (3, 4, 26, 29). We have also shown that

increasing cardiomyocyte *O*-GlcNAc levels was associated with a decrease in angiotensin II-induced increases in cytosolic Ca^{2+} entry (28). Therefore, in light of the fact that STIM1 is now recognized as a key player in regulating SOCE, we postulated that increased *O*-GlcNAcylation would interfere with normal STIM1 function.

We first demonstrated that STIM1 was present in the adult rat heart and co-localized with SERCA and RyR, indicating localization to the SR, which is in agreement with accepted models of SOCE in non-excitable cells as well as recent reports of STIM1 in cardiomyocytes (19, 20, 21) and skeletal muscle (46). A key feature of STIM1 mediated SOCE is the formation of STIM1 oligomers in the ER membrane; therefore to determine

the effects of increased *O*-GlcNAc levels on STIM1 function, we first transfected neonatal cardiomyocytes with eYFP-STIM1 and demonstrated that treatment with EGTA and thapsigargin to trigger depletion of SR Ca^{2+}, resulted in the rapid formation of STIM1 puncta and subsequent co-localization with Orai1 (Fig. 2). Under control conditions EGTA and thapsigargin treatment resulted in ~90% of cells becoming STIM1 puncta positive; however, increasing *O*-GlcNAc levels with either or thiamet-G, significantly attenuated both the number of puncta positive cells and the average number of STIM1 puncta per cell (Fig. 3). The fact that the EC_{50} for increasing O-GlcNAc and decreasing STIM1 puncta formation were similar for glucosamine (~150–200 μM) and thiamet-G (70–100 nM) provided further support for a link between O-GlcNAcylation and regulation of STIM1 function (Fig. 4). It should be noted that these experiments were not designed to determine the effects of *O*-GlcNAcylation on the rates of puncta formation or their reversibility; clearly such studies would provide valuable additional insight in the mechanisms by which O-GlcNAc modulates STIM1 function.

Furthermore, attenuation of STIM1 puncta formation by both glucosamine and thiamet-G also blunted subsequent entry of Ca^{2+} (Fig. 5A), On the other hand, glucosamine had no effect on voltage gated Ca^{2+} entry induced by depolarization of the cells with high K^+, demonstrating that the effects of glucosamine and by inference *O*-GlcNAc are specific for STIM1-mediated Ca^{2+} entry with no direct affect on voltage-gated Ca^{2+} entry (Fig. 5B). Voltage-gated Ca^{2+} entry mediated by L-type Ca^{2+} channels play a central role in excitation-contraction coupling; therefore, these results are also consistent with the fact that in the intact perfused heart neither glucosamine nor OGA inhibitors had an effect on contractility (29, 30, 34, 35).

In skeletal muscle, the L-type Ca^{2+} channel-dependent excitation-coupled calcium entry (ECCE) was observed in response to SOCE (47–49). However, in NRVMs, L-type Ca^{2+} channel inhibitors verapamil and nifedipine, had no effect on SOCE (3), suggesting that in this cell type at least, SOCE does not trigger further Ca^{2+} entry via voltage gated Ca^{2+} channels. Interestingly, although Orai1 is intrinsically a non-selective cation channel, STIM1 has recently been shown not only to gate Orai1 upon SOCE stimulation but also regulate its ion selectivity through direct interaction (50). Therefore, the fact that in NRVMs SOCE is highly Ca^{2+} selective (Fig. 5D) supports the concept that it is triggered by a STIM1-Orai1-coupled process; this is consistent with earlier report that both STIM1 and Orai1 play a key role in cardiomyocyte SOCE (21).

Orai1 and TRPC have both been reported as SOC channels; however, their activation and involvement during SOCE remain unresolved. Although STIM1 interacts with both Orai1 and TRPC channels it activates TRPC through its polylysine domain and Orai1 through the SOAR domain, thereby allowing both channels to function independently. SOCE has shown to be Sr^{2+}-permeable and thus TRPC-mediated in RBL-2H3 (51), vascular smooth muscle cells (52), and skeletal myotubes (47), but not in astrocytes (53), C6 cells or A7r5 cells (41). These studies clearly indicate that the relative contributions of Orai1 and TRPCs to SOCE are cell type specific. Interestingly, in adult

cardiomyocytes Hulot *et al.*, observed that SOCE was non-selective (20), suggesting that the SOC channel activation might be not only cell-type but also development dependent.

While it is well accepted that STIM1 is essential for SOCE, the mechanism(s) that regulate its function and are necessary for leading to STIM1 oligomerization are less well understood. However, the cytosolic C-terminal region of STIM1 contains a PEST sequence (55), which is a region that has a high potential for O-GlcNAcylation. We demonstrated that there is a basal level of *O*-GlcNAcylation of STIM1 and both glucosamine and thiamet-G increased STIM1 *O*-GlcNAc levels (Fig. 6, *A* and *C*). Previously it has been shown in HEK293 cells that activation of STIM1-mediated Ca^{2+} entry was dependent on ERK1/2 phosphorylation of STIM1 (42); here we demonstrated that this is also true in cardiomyocytes (Fig. 6D). We also found that while thiamet-G treatment prevented the thapsigargin-induced increase in STIM1 phosphorylation, thiamet-G also increased basal STIM1 phosphorylation. Further studies are clearly needed to better understand the interactions between STIM1 phosphorylation and *O*-GlcNAcylation; nevertheless, these data support the notion that the attenuation of STIM1 puncta formation and SOCE by glucosamine and thiamet-G was due to increased *O*-GlcNAc modification of STIM1 and that increasing STIM1 *O*-GlcNAcylation alters the regulation of STIM1 phosphorylation.

The goal of this study was to determine the effects of *O*-GlcNAc on STIM1 puntca formation and STIM1-mediated SOCE. Since STIM1 puncta formation is required for SOCE activation, the attenuation of SOCE, observed with glucosamine or thiamet-G pretreatment, could be attributed partially, if not entirely due to their effects of increased *O*-GlcNAc levels on STIM1. However, we also cannot rule out the possibility that increased cellular *O*-GlcNAc levels could also modulate the interaction between STIM1 and Orai1 or directly modify Orai1 or other components of the macromolecular SOC complex. It is also worth noting that there are several potential phosphorylation sites on Orai1 (56) and that the cytoplasmic domains of Orai1 have been reported interact with many other proteins, including calmodulin (57), Golli (58), and Ca^{2+}-ATPases (59, 60). It is clear therefore, that *O*-GlcNAcylation has the potential to regulate Orai1 function either directly or via modification its partners. Additional studies such as the effect of altered *O*-GlcNAc levels on CRAC currents could provide some insights into whether increased *O*-GlcNAc levels might have a direct effect on Orai1 function.

A role for STIM1-mediated Ca^{2+} signaling in excitable cells including cardiac and skeletal myocytes (61, 62), neurons (63) and pancreatic β-cells (64) is gradually being appreciated; however, to our knowledge this is the first study to demonstrate that STIM1 is a target for *O*-GlcNAc modification and that this is associated with impaired STIM1 function and blunted SOCE. This has implications not only for our understanding of the regulation of STIM1 function under normal physiological conditions, but also provides new insights into the how changes in cellular *O*-GlcNAc levels affect cellular stress responses. For example, we have demonstrated that acute increases in *O*-GlcNAc prevent Ca^{2+} overload induced by the Ca^{2+} paradox and ischemia/reperfusion injury. The Na^+/Ca^{2+}

exchanger and L-type Ca^{2+} channels are typically associated with mediating Ca^{2+} overload in the heart; however, recent studies in the intact heart showed that during early reperfusion there was a significant drop in SR Ca^{2+} (65), which would be a trigger for STIM1 oligomerization. It is conceivable therefore that *O*-GlcNAc modification of STIM1 could be a contributing factor to the acute cytoprotective effects of increased *O*-GlcNAcylation.

It is also of note that NFAT translocation, which we have previously demonstrated to be mediated by SOCE (3) and is essential for activation the hypertrophic transcriptional pathways, has recently been reported to be *O*-GlcNAc-dependent (66). Furthermore, in hearts and cardiomyocytes from diabetic animals we have shown that the contractile and hypertrophic signaling responses to angiotensin II and phenylephrine are significantly blunted (25, 29). Since diabetes leads to chronically increased cardiomyocyte *O*-GlcNAc levels (25, 54), it is entirely possible that *O*-GlcNAcylation of STIM1 represents another mechanism contributing to the adverse effects of diabetes. This is also consistent with the observation that platelets from type 2 diabetic patients exhibit blunted SOCE, which was linked to impaired association between STIM1, Orai1, and hTRPC1/6 (45). Consequently, these findings also have potential implications for understanding the adverse effects of diabetes on Ca^{2+} signaling in other cell types.

Taken together these data support the notion that activation of cardiomyocyte *O*-GlcNAcylation attenuates SOCE via *O*-GlcNAc modification of STIM1 and that this may represent a novel mechanism underlying both the acute cytoprotective effects of increased *O*-GlcNAcylation as well as the adverse effects of increased *O*-GlcNAc levels associated with diabetes and aging. Further studies are clearly needed to identify the specific sites of STIM1 *O*-GlcNAcylation and to better understand the interrelationship between regulation of STIM1 function by *O*-GlcNAcylation and phosphorylation. Nevertheless, given that SOCE is a fundamental mechanism underlying Ca^{2+} signaling in most cells and tissues, it is possible that STIM1 represent a critical nexus linking protein *O*-GlcNAcylation with Ca^{2+}-mediated transcription.

REFERENCES

1. Feske, S., Picard, C., and Fischer, A. (2010) Immunodeficiency due to mutations in ORAI1 and STIM1. *Clin. Immunol.* **135,** 169–182
2. Baba, Y., and Kurosaki, T. (2009) Physiological function and molecular basis of STIM1-mediated calcium entry in immune cells. *Immunol. Rev.* **231,** 174–188
3. Hunton, D. L., Lucchesi, P. A., Pang, Y., Cheng, X., Dell'Italia, L. J., and Marchase, R. B. (2002) Capacitative calcium entry contributes to nuclear factor of activated T-cells nuclear translocation and hypertrophy in cardiomyocytes. *J. Biol. Chem.* **277,** 14266–14273
4. Pang, Y., Hunton, D. L., Bounelis, P., and Marchase, R. B. (2002) Hyperglycemia inhibits capacitative calcium entry and hypertrophy in neonatal cardiomyocytes. *Diabetes* **51,** 3461–3467
5. Uehara, A., Yasukochi, M., Imanaga, I., Nishi, M., and Takeshima, H. (2002) Store-operated Ca2+ entry uncoupled with ryanodine receptor and junctional membrane complex in heart muscle cells. *Cell Calcium* **31,** 89–96
6. Hunton, D. L., Zou, L., Pang, Y., and Marchase, R. B. (2004) Adult rat cardiomyocytes exhibit capacitative calcium entry. *Am. J. Physiol. Heart Circ. Physiol.* **286,** H1124–H1132
7. Cheng, K. T., Ong, H. L., Liu, X., and Ambudkar, I. S. Contribution of TRPC1 and Orai1 to Ca(2+) entry activated by store depletion. *Adv. Exp. Med. Biol.* **704,** 435–449
8. Roos, J., DiGregorio, P. J., Yeromin, A. V., Ohlsen, K., Lioudyno, M., Zhang, S., Safrina, O., Kozak, J. A., Wagner, S. L., Cahalan, M. D., Veliçelebi, G., and Stauderman, K. A. (2005) STIM1, an essential and conserved component of store-operated Ca^{2+} channel function. *J. Cell Biol.* **169,** 435–445
9. Liou, J., Kim, M. L., Heo, W. D., Jones, J. T., Myers, J. W., Ferrell, J. E., Jr., and Meyer, T. (2005) STIM is a Ca^{2+} sensor essential for Ca^{2+}-store-depletion-triggered Ca^{2+} influx. *Curr. Biol.* **15,** 1235–1241
10. Zhang, S. L., Yeromin, A. V., Zhang, X. H., Yu, Y., Safrina, O., Penna, A., Roos, J., Stauderman, K. A., and Cahalan, M. D. (2006) Genome-wide RNA_i screen of Ca(2+) influx identifies genes that regulate Ca(2+) release-activated Ca(2+) channel activity. *Proc. Natl. Acad. Sci. U.S.A.* **103,** 9357–9362
11. Soboloff, J., Spassova, M. A., Tang, X. D., Hewavitharana, T., Xu, W., and Gill, D. L. (2006) Orai1 and STIM reconstitute store-operated calcium channel function. *J. Biol. Chem.* **281,** 20661–20665
12. Deng, X., Wang, Y., Zhou, Y., Soboloff, J., and Gill, D. L. (2009) STIM and Orai: dynamic intermembrane coupling to control cellular calcium signals. *J. Biol. Chem.* **284,** 22501–22505
13. Wang, Y., Deng, X., Zhou, Y., Hendron, E., Mancarella, S., Ritchie, M. F., Tang, X. D., Baba, Y., Kurosaki, T., Mori, Y., Soboloff, J., and Gill, D. L. (2009) STIM protein coupling in the activation of Orai channels. *Proc. Natl. Acad. Sci. U.S.A.* **106,** 7391–7396
14. Cahalan, M. D. (2009) STIMulating store-operated Ca(2+) entry. *Nat. Cell Biol.* **11,** 669–677
15. Salido, G. M., Jardin, I., and Rosado, J. A. (2011) The TRPC ion channels: association with Orai1 and STIM1 proteins and participation in capacitive and non-capacitative calcium entry. *Adv. Exp. Med. Biol.* **704,** 413–433
16. Wu M. M., Buchanan, J., Luik, R. M., and Lewis, R. S. (2006) Ca^{2+} store depletion causes STIM1 to accumulate in ER regions closely associated with the plasma membrane. *J. Cell Biol.* **174,** 803–813
17. Lewis, R. S. (2007) The molecular choreography of a store-operated calcium channel. *Nature* **446,** 284–287
18. Yeromin, A. V., Zhang, S. L., Jiang, W., Yu, Y., Safrina, O., and Cahalan, M. D. (2006) Molecular identification of the CRAC channel by altered ion selectivity in a mutant of Orai. *Nature* **443,** 226–229
19. Luo, X., Hojayev, B., Jiang, N., Wang, Z. V., Tandan, S., Rakalin, A., Rothermel, B. A., Gillette, T. G., and Hill, J. A. (2012) STIM1-dependent store-operated Ca(2)(+) entry is required for pathological cardiac hypertrophy. *J. Mol. Cell Cardiol.* **52,** 136–147
20. Hulot, J. S., Fauconnier, J., Ramanujam, D., Chaanine, A., Aubart, F., Sassi, Y., Merkle, S., Cazorla, O., Ouille, A., Dupuis, M., Hadri, L., Jeong, D., Mühlstedt, S., Schmitt, J., Braun, A., Bénard, L., Saliba, Y., Laggerbauer, B., Nieswandt, B., Lacampagne, A., Hajjar, R. J., Lompré, A. M., and Engelhardt, S. (2011) Critical role for stromal interaction molecule 1 in cardiac hypertrophy. *Circulation* **124,** 796–805
21. Voelkers, M., Salz, M., Herzog, N., Frank, D., Dolatabadi, N., Frey, N., Gude, N., Friedrich, O., Koch, W. J., Katus, H. A., Sussman, M. A., and Most, P. (2010) Orai1 and Stim1 regulate normal and hypertrophic growth in cardiomyocytes. *J. Mol. Cell Cardiol.* **48,** 1329–1334
22. Ohba, T., Watanabe, H., Murakami, M., Sato, T., Ono, K., and Ito, H. (2009) Essential role of STIM1 in the development of cardiomyocyte hypertrophy. *Biochem. Biophys. Res. Commun.* **389,** 172–176
23. Rosenberg, P. (2011) Socking it to cardiac hypertrophy: STIM1-mediated Ca^{2+} entry in the cardiomyocyte. *Circulation* **124,** 766–768
24. Zachara, N. E., O'Donnell, N., Cheung, W. D., Mercer, J. J., Marth, J. D., and Hart, G. W. (2004) Dynamic *O*-GlcNAc modification of nucleocytoplasmic proteins in response to stress. A survival response of mammalian cells. *J. Biol. Chem.* **279,** 30133–30142
25. Marsh, S. A., Dell'Italia, L. J., and Chatham, J. C. (2011) Activation of the

hexosamine biosynthesis pathway and protein *O*-GlcNAcylation modulate hypertrophic and cell signaling pathways in cardiomyocytes from diabetic mice. *Amino Acids* **40,** 819–828

26. Darbha, S., and Marchase, R. B. (1996) Regulation of intracellular calcium is closely linked to glucose metabolism in J774 macrophages. *Cell Calcium* **20,** 361–371

27. Rivera, A. A., White, C. R., Guest, L. L., Elton, T. S., and Marchase, R. B. (1995) Hyperglycemia alters cytoplasmic Ca^{2+} responses to capacitative Ca^{2+} influx in rat aortic smooth muscle cells. *Am. J. Physiol.* **269,** C1482–C1488

28. Nagy, T., Champattanachai, V., Marchase, R. B., and Chatham, J. C. (2006) Glucosamine inhibits angiotensin II-induced cytoplasmic Ca^{2+} elevation in neonatal cardiomyocytes via protein-associated *O*-linked *N*-acetylglucosamine. *Am. J. Physiol. Cell Physiol.* **290,** C57–C65

29. Pang, Y., Bounelis, P., Chatham, J. C., and Marchase, R.B. (2004) Hexosamine pathway is responsible for inhibition by diabetes of phenylephrine-induced inotropy. *Diabetes* **53,** 1074–1081

30. Laczy, B., Marsh, S. A., Brocks, C. A., Wittmann, I., and Chatham, J. C. (2010) Inhibition of *O*-GlcNAcase in perfused rat hearts by NAG-thiazolines at the time of reperfusion is cardioprotective in an *O*-GlcNAc-dependent manner. *Am. J. Physiol. Heart Circ. Physiol.* **299,** H1715–H1727

31. Champattanachai, V., Marchase, R. B., and Chatham, J. C. (2008) Glucosamine protects neonatal cardiomyocytes from ischemia-reperfusion injury via increased protein *O*-GlcNAc and increased mitochondrial Bcl-2. *Am. J. Physiol. Cell Physiol* **294,** C1509–C1520

32. Liu, J., Marchase, R. B., and Chatham, J. C. (2007) Increased *O*-GlcNAc levels during reperfusion lead to improved functional recovery and reduced calpain proteolysis. *Am. J. Physiol. Heart Circ. Physiol.* **293,** H1391–H1399

33. Yuzwa, S. A., Macauley, M. S., Heinonen, J. E., Shan, X., Dennis, R. J., He, Y., Whitworth, G. E., Stubbs, K. A., McEachern, E. J., Davies, G. J., and Vocadlo, D. J. (2008) A potent mechanism-inspired *O*-GlcNAcase inhibitor that blocks phosphorylation of tau *in vivo*. *Nat. Chem. Biol.* **4,** 483–490

34. Fülöp, N., Zhang, Z., Marchase, R. B., and Chatham, J. C. (2007) Glucosamine cardioprotection in perfused rat hearts associated with increased *O*-linked *N*-acetylglucosamine protein modification and altered p38 activation. *Am. J. Physiol. Heart Circ. Physiol.* **292,** H2227–H2236

35. Liu, J., Pang, Y., Chang, T., Bounelis, P., Chatham, J. C., and Marchase, R. B. (2006) Increased hexosamine biosynthesis and protein *O*-GlcNAc levels associated with myocardial protection against calcium paradox and ischemia. *J. Mol. Cell Cardiol.* **40,** 303–312

36. Lee, K. P., Yuan, J. P., Hong, J. H., So, I., Worley, P. F., and Muallem, S. (2010) An endoplasmic reticulum/plasma membrane junction: STIM1/Orai1/TRPCs. *FEBS Lett.* **584,** 2022–2027

37. Liao, Y., Erxleben, C., Abramowitz, J., Flockerzi, V., Zhu, M. X., Armstrong, D. L., and Birnbaumer, L. (2008) Functional interactions among Orai1, TRPCs, and STIM1 suggest a STIM-regulated heteromeric Orai/TRPC model for SOCE/Icrac channels. *Proc. Natl. Acad. Sci. U.S.A.* **105,** 2895–2900

38. Nilius, B., Owsianik, G., Voets, T., and Peters, J. A. (2007) Transient receptor potential cation channels in disease. *Physiol. Rev.* **87,** 165–217

39. Feske, S., Gwack, Y., Prakriya, M., Srikanth, S., Puppel, S. H., Tanasa, B., Hogan, P. G., Lewis, R. S., Daly, M., and Rao, A. (2006) A mutation in Orai1 causes immune deficiency by abrogating CRAC channel function. *Nature* **441,** 179–185

40. Vig, M., Peinelt, C., Beck, A., Koomoa, D. L., Rabah, D., Koblan-Huberson, M., Kraft, S., Turner, H., Fleig, A., Penner, R., and Kinet, J. P. (2006) CRACM1 is a plasma membrane protein essential for store-operated Ca2+ entry. *Science* **312,** 1220–1223

41. Wang, Y., Deng, X., Mancarella, S., Hendron, E., Eguchi, S., Soboloff, J., Tang, X. D., and Gill, D. L. (2010) The calcium store sensor, STIM1, reciprocally controls Orai and CaV1.2 channels. *Science* **330,** 105–109

42. Pozo-Guisado, E., Campbell, D. G., Deak, M., Alvarez-Barrientos, A., Morrice, N. A., Alvarez, I. S., Alessi, D. R., and Martin-Romero, F. J. (2010) Phosphorylation of STIM1 at ERK1/2 target sites modulates store-operated calcium entry. *J. Cell Science* **123,** 3084–3093

43. Vaca, L. (2010) SOCIC: the store-operated calcium influx complex. *Cell Calcium* **47,** 199–209

44. Bers, D. M. (2008) Calcium cycling and signaling in cardiac myocytes. *Annu. Rev. Physiol.* **70,** 23–49

45. Jardin, I., Lopez, J. J., Zbidi, H., Bartegi, A., Salido, G. M., and Rosado, J. A. (2011) Attenuated store-operated divalent cation entry and association between STIM1, Orai1, hTRPC1, and hTRPC6 in platelets from type 2 diabetic patients. *Blood Cells Mol Dis.* **46,** 252–260

46. Dirksen, R. T. (2009) Checking your SOCCs and feet: the molecular mechanisms of Ca^{2+} entry in skeletal muscle. *J. Physiol.* **587,** 3139–3147

47. Cherednichenko, G., Hurne, A. M., Fessenden, J. D., Lee, E. H., Allen, P. D., Beam, K. G., and Pessah, I. N. (2004) Conformational activation of Ca^{2+} entry by depolarization of skeletal myotubes. *Proc. Natl. Acad. Sci. U.S.A.* **101,** 15793–15798

48. Bannister, R. A., Colecraft, H. M., and Beam, K. G. (2008) Rem inhibits skeletal muscle EC coupling by reducing the number of functional L-type Ca^{2+} channels. *Biophys J.* **94,** 2631–2638

49. Bannister, R. A., and Beam, K. G. (2009) The cardiac $\alpha(1C)$ subunit can support excitation-triggered Ca^{2+} entry in dysgenic and dyspedic myotubes. *Channels* **3,** 268–273

50. McNally, B. A., Somasundaram, A., Yamashita, M., and Prakriya, M. (2012) Gated regulation of CRAC channel ion selectivity by STIM1. *Nature* **482,** 241–245

51. Ma, H. T., Peng, Z., Hiragun, T., Iwaki, S., Gilfillan, A. M., and Beaven, M. A. (2008) Canonical transient receptor potential 5 channel in conjunction with Orai1 and STIM1 allows Sr^{2+} entry, optimal influx of Ca^{2+}, and degranulation in a rat mast cell line. *J. Immunol.* **180,** 2233–2239

52. Trepakova, E. S., Gericke, M., Hirakawa, Y., Weisbrod, R. M., Cohen, R. A., and Bolotina, V. M. (2001) Properties of a native cation channel activated by Ca^{2+} store depletion in vascular smooth muscle cells. *J. Biol. Chem.* **276,** 7782–7790

53. Grimaldi, M., Maratos, M., and Verma, A. (2003) Transient receptor potential channel activation causes a novel form of $[Ca^{2+}]I$ oscillations and is not involved in capacitative Ca^{2+} entry in glial cells. *J. Neurosci.* **23,** 4737–4745

54. Fülöp, N., Mason, M. M., Dutta, K., Wang, P., Davidoff, A. J., Marchase, R. B., and Chatham, J. C. (2007) Impact of Type 2 diabetes and aging on cardiomyocyte function and *O*-linked *N*-acetylglucosamine levels in the heart. *Am. J. Physiol. Cell Physiol* **292,** C1370–C1378

55. Várnai, P., Hunyady, L., and Balla, T. (2009) STIM and Orai: the long-awaited constituents of store-operated calcium entry. *Trends Pharmacol. Sci.* **30,** 118–128

56. Hewavitharana, T., Deng, X., Soboloff, J., and Gill, D. L. (2007) Role of STIM and Orai proteins in the store-operated calcium signaling pathway. *Cell Calcium* **42,** 173–182

57. Mullins, F. M., Park, C. Y., Dolmetsch, R. E., and Lewis, R. S. (2009) STIM1 and calmodulin interact with Orai1 to induce Ca^{2+}-dependent inactivation of CRAC channels. *Proc. Natl. Acad. Sci. U.S.A.* **106,** 15495–15500

58. Walsh, C. M., Doherty, M. K., Tepikin, A. V., and Burgoyne, R. D. (2010) Evidence for an interaction between Golli and STIM1 in store-operated calcium entry. *Biochem. J.* **430,** 453–460

59. Feng, M., Grice, D. M., Faddy, H. M., Nguyen, N., Leitch, S., Wang, Y., Muend, S., Kenny, P. A., Sukumar, S., Roberts-Thomson, S. J., Monteith, G. R., and Rao, R. (2010) Store-independent activation of Orai1 by SPCA2 in mammary tumors. *Cell* **143,** 84–98

60. Quintana, A., Pasche, M., Junker, C., Al-Ansary, D., Rieger, H., Kummerow, C., Nunez, L., Villalobos, C., Meraner, P., and Becherer, U. (2011) Calcium microdomains at the immunological synapse: how ORAI channels, mitochondria and calcium pumps generate local calcium signals for efficient T-cell activation. *EMBO J.* **30,** 3895–3912

61. Stiber, J. A., and Rosenberg, P.B. (2011) The role of store-operated calcium influx in skeletal muscle signaling. *Cell Calcium* **49,** 341–349

62. Lyfenko, A. D., and Dirksen, R. T. (2008) Differential dependence of store-operated and excitation-coupled Ca^{2+} entry in skeletal muscle on STIM1 and Orai1. *J. Physiol.* **586,** 4815–4824

63. Gruszczynska-Biegala, J., Pomorski, P., Wisniewska, M. B., and Kuznicki, J.

(2011) Differential roles for STIM1 and STIM2 in store-operated calcium entry in rat neurons. *PLoS One* **6,** e19285

64. Tamarina, N. A., Kuznetsov, A., and Philipson, L. H. (2008) Reversible translocation of EYFP-tagged STIM1 is coupled to calcium influx in insulin secreting beta-cells. *Cell Calcium* **44,** 533–544

65. Valverde, C. A., Kornyeyev, D., Ferreiro, M., Petrosky, A. D., Mattiazzi, A., and Escobar, A. L. (2010) Transient Ca^{2+} depletion of the sarco-plasmic reticulum at the onset of reperfusion. *Cardiovasc. Res.* **85,** 671–680

66. Facundo, H. T., Brainard, R. E., Watson, L. J., Ngoh, G. A., Hamid, T., Prabhu, S. D., and Jones, S. P. (2012) *O*-GlcNAc signaling is essential for NFAT-mediated transcriptional reprogramming during cardiomyocyte hypertrophy. *Am. J. Physiol. Heart Circul. Physiol.* **302,** H2122–H2130